

Thermal buckling analysis of shear deformable laminated orthotropic plates by differential quadrature

S. Moradi*¹ and Mohammad Hassan Mansouri²

¹Mechanical Engineering Department, Shahid Chamran University, Ahvaz, 61355, Iran

²NIGC, Isfahan, P.O.Box 85865-1111, Iran

(Received August 06, 2010, Revised November 10, 2010, Accepted November 16, 2011)

Abstract. In this paper, the thermal buckling analysis of rectangular composite laminated plates is investigated using the Differential Quadrature (DQ) method. The composite plate is subjected to a uniform temperature distribution and arbitrary boundary conditions. The analysis takes place in two stages. First, pre-buckling forces due to a temperature rise are determined by using a membrane solution. In the second stage, the critical temperature is predicted based on the first-order shear deformation theory. To verify the accuracy of the method, several case studies were used and the numerical results were compared with those of other published literatures. Moreover, the effects of several parameters such as aspect ratio, fiber orientation, modulus ratio, and various boundary conditions on the critical temperature were examined. The results confirm the efficiency and accuracy of the DQ method in dealing with this class of engineering problems.

Keywords: thermal buckling; differential quadrature; shear deformation theory; composite plates.

1. Introduction

Laminated composites, which have high strength-to-weight and stiffness-to-weight ratios and diversity, have been used extensively in important applications ranging from aerospace to automobile industries. In some applications, these structural components are under high temperature and thermal gradient environments. As a result, with certain types of boundary conditions, these components are susceptible to thermal buckling. The thermal buckling of composite laminated plates is one of practical importance for structures operating at elevated temperatures and therefore, there have been continued research interests on the topic in recent years.

The thermal buckling of thick symmetric angle-ply laminates were analyzed by Huang and Tauchert (1992) based on the first-order shear deformation theory by using a Fourier series and the finite element method. Sun and Hsu (1990) produced a close-form solution for the thermal buckling of simply supported, symmetric cross-ply laminates, taking into account the through-thickness shearing action. Prabhu and Dhanaraj (1994) considered the thermal buckling of laminated composite plates subject to a uniform temperature rise using finite element method in the context of shear deformation plate theory (SDPT). Chen *et al.* (1991) and Thangaratnam *et al.* (1989) have also conducted such studies but with non-uniform temperature fields. The critical buckling temperature of symmetric and anti-symmetric composite

* Corresponding author, Ph. D., E-mail: moradis@scu.ac.ir,

plates subject to uniform and non-uniform temperature variations were analyzed by Dawe and Ge (2000). They used finite strip method based on a first order shear deformation theory (FSDT). Kant and Babu (2000) used first and higher order shear deformable finite elements model to obtain the thermal buckling of skew fiber-reinforced composite and sandwich plates. Based on a FSDT Prakash *et al.* (2006) investigated the axisymmetric free vibration and thermal stability behavior of functionally graded spherical caps by a three noded curved shell element. Matsunaga (2006 and 2007) used a two-dimensional global higher order deformation theory to evaluate the buckling temperature in laminated composite angle-ply plates and cross-ply shallow shells by using the method of power series expansion. Based on double Fourier series, an analytical solution for the thermal buckling of thick symmetric angle-ply laminated plates under clamped boundary conditions was obtained by Kabir *et al.* (2007). Shariyat (2007) used a layerwise plate theory and finite elements method to study the thermal buckling of rectangular composite plates under uniform temperature rise. Shiau *et al.* (2010) studied the thermal buckling behavior of composite laminated cross-ply and angle-ply plates using a higher order triangular plate element.

Bellman and Casti (1971) introduced the differential quadrature method in early seventies. It is based on the weighted sum of function values as an approximation to the derivatives of that function. Since then, several researchers have applied the method to solve varieties of problems in different areas of science and technology (Bert and Malik (1996), Hakimi and Moradi (2010), Hu *et al.* (2009), Karami and Malekzadeh (2006)). Using a higher order shear deformation theory Li and Cheng (2005) solved the problem of nonlinear vibration of orthotropic plates with finite deformation by DQ method. Farid *et al.* (2010) studied the three-dimensional temperature dependent free vibration of functionally graded material curved panels using a hybrid semi-analytic DQ method. The method has been shown to be a powerful contender in solving systems of differential equations. Therefore, it has become an alternative to the existing numerical methods such as finite difference and finite element methods.

The non-linear bending analysis of plates under the thermal load was investigated by Lin *et al.* (1994). Jane and Hong (2000) used the DQ method to analyze the bending of simply supported rectangular thin symmetric cross-ply laminated plates subject to a uniform thermal load and a uniform pressure. They have also studied the thermal analysis of simply supported, cross-ply and angle-ply laminated composite plates subjected to a sinusoidal thermal load based on FSDT (2003).

To the authors' best knowledge, the validity of DQ method in treating the thermal buckling of laminated composite plates has not yet been explored. Hence, in this study, the DQ method is applied to analyze the bifurcation buckling of rectangular composite plates for predicting the critical temperature. The integrity of the method is verified through several case studies. The effects of several parameters, such as aspect ratio, fiber orientation, modulus ratio, as well as various boundary conditions are also investigated.

2. Thermal buckling

Consider a laminated composite plate having NL layers. The geometry of the plate is shown in Fig. 1. Here a , b and h are the length, width and the thickness of the plate, respectively. Each layer is considered to be homogeneous and orthotropic. It is assumed that the temperature is constant through the thickness and its changes are measured from the stress-free state. Moreover, the material properties are independent of temperature variations. It is further assumed that after the thermal load is applied, the plate remains flat until the temperature reaches its critical value. Then, the buckling occurs and the

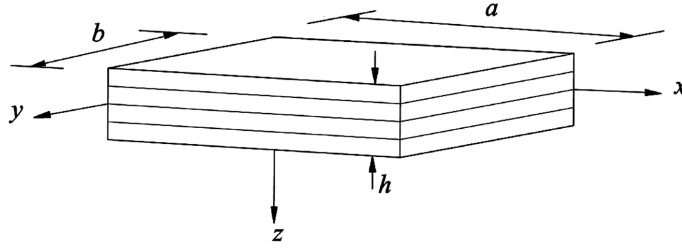


Fig. 1 Geometry of a composite laminated plate.

plate bifurcates. It should be noted that, an eigenvalue analysis cannot be carried out for every composite laminated plate and there are some limitations on the type of lamination, which result in a bifurcation buckling (Prabhu and Dhanaraj (1994), Dawe and Ge (2000), Leissa (1986), Qatu and Leissa (1993)).

In order to account for shear deformation effects in the plate, the displacement components are taken as

$$\begin{aligned} u &= u_0 + z \psi_x \\ v &= v_0 + z \psi_y \\ w &= w_0 \end{aligned} \quad (1)$$

where u_0 , v_0 and w_0 are associated mid-plane displacements in the x , y and z directions and, ψ_x and ψ_y are the rotations of a transverse normal about the y and x axes, respectively. The coordinate frame is chosen in such a way that the xy plane coincides with the mid-plane of the plate.

The strain-displacement relations are defined as

$$\begin{aligned} \varepsilon_x &= u_{0,x} + z \psi_{x,y} \\ \varepsilon_y &= v_{0,y} + z \psi_{y,y} \\ \gamma_{xy} &= u_{0,y} + v_{0,x} + z (\psi_{x,y} + \psi_{y,x}) \\ \gamma_{zx} &= w_{0,x} + \psi_x \\ \gamma_{zy} &= w_{0,y} + \psi_y \end{aligned} \quad (2)$$

here ε_x and ε_y are normal strains and, γ_{xy} , γ_{zx} and γ_{zy} are shear strains, respectively. Furthermore, in the presence of a temperature rise ΔT , the thermal strains are expressed as

$$\begin{aligned} \varepsilon_x^T &= \Delta T \alpha_x \\ \varepsilon_y^T &= \Delta T \alpha_y \\ \gamma_{xy}^T &= \Delta T \alpha_{xy} \end{aligned} \quad (3)$$

where the thermal strains are shown by ε^T and, α_x , α_y and α_{xy} are thermal expansion coefficients. Then, based on generalized Hook's law, the stress-strain relationship of each lamina is given by (Whitney (1987))

$$\begin{pmatrix} \sigma_x \\ \sigma_y \\ \sigma_{xy} \end{pmatrix}^{(k)} = \begin{pmatrix} \bar{Q}_{11} & \bar{Q}_{12} & \bar{Q}_{16} \\ \bar{Q}_{12} & \bar{Q}_{22} & \bar{Q}_{26} \\ \bar{Q}_{16} & \bar{Q}_{26} & \bar{Q}_{66} \end{pmatrix}^{(k)} \begin{pmatrix} \varepsilon_x - \varepsilon_x^T \\ \varepsilon_y - \varepsilon_y^T \\ \varepsilon_{xy} - \varepsilon_{xy}^T \end{pmatrix}^{(k)}$$

$$\begin{pmatrix} \sigma_{zy} \\ \sigma_{zx} \end{pmatrix}^{(k)} = \begin{pmatrix} \bar{Q}_{44} & \bar{Q}_{45} \\ \bar{Q}_{45} & \bar{Q}_{55} \end{pmatrix}^{(k)} \begin{pmatrix} \gamma_{zy} \\ \gamma_{zx} \end{pmatrix}^{(k)} \quad (4)$$

here the superscript k denotes k th layer, σ_i and \bar{Q}_{ij} are stress components and transformed stiffness matrix coefficients related to the k th layer, respectively.

Stress resultants, as shown in Fig. 2, are defined as

$$\begin{pmatrix} N_x \\ N_y \\ N_{xy} \end{pmatrix} = \int_{-\frac{h}{2}}^{\frac{h}{2}} \begin{pmatrix} \sigma_x \\ \sigma_y \\ \sigma_{xy} \end{pmatrix}^{(k)} dz$$

$$\begin{pmatrix} M_x \\ M_y \\ M_{xy} \end{pmatrix} = \int_{-\frac{h}{2}}^{\frac{h}{2}} \begin{pmatrix} \sigma_x \\ \sigma_y \\ \sigma_{xy} \end{pmatrix}^{(k)} z dz$$

$$\begin{pmatrix} Q_y \\ Q_x \end{pmatrix} = \int_{-\frac{h}{2}}^{\frac{h}{2}} \begin{pmatrix} \sigma_y \\ \sigma_{zx} \end{pmatrix}^{(k)} dz \quad (5)$$

where N_x , N_y and N_{xy} are in-plane forces per unit length, M_x , M_y and M_{xy} are the bending and torsional moments per unit length, and Q_x and Q_y are transverse shear forces per unit length, respectively. After substituting Eq. (4) into Eq. (5), and performing the indicated integrations, the stress resultants can be expressed as

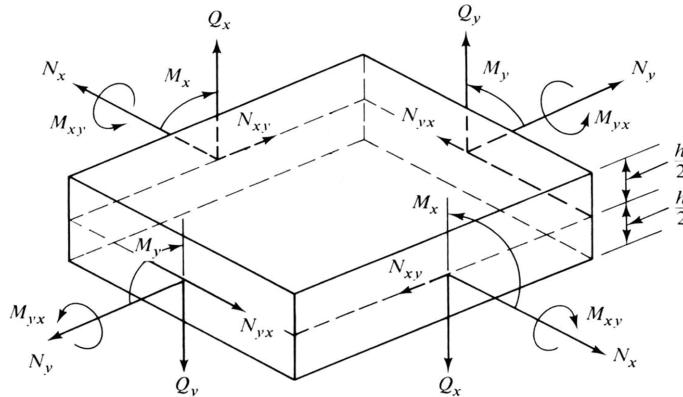


Fig. 2 Stress resultant in a plate element

$$\begin{pmatrix} N_x \\ N_y \\ N_{xy} \\ M_x \\ M_y \\ M_{xy} \end{pmatrix} = \begin{pmatrix} A_{11} & A_{12} & A_{16} & B_{11} & B_{12} & B_{16} \\ & A_{22} & A_{26} & B_{12} & B_{22} & B_{26} \\ & & A_{66} & B_{16} & B_{26} & B_{66} \\ & & & D_{11} & D_{12} & D_{16} \\ \text{Sym.} & & & & D_{22} & D_{26} \\ & & & & & D_{66} \end{pmatrix} \begin{pmatrix} u_{0,x} \\ v_{0,y} \\ u_{0,y} + v_{0,x} \\ \psi_{x,x} \\ \psi_{y,y} \\ \psi_{x,y} + \psi_{y,x} \end{pmatrix} - \begin{pmatrix} N_x^T \\ N_y^T \\ N_{xy}^T \\ 0 \\ 0 \\ 0 \end{pmatrix}$$

$$\begin{pmatrix} Q_y \\ Q_x \end{pmatrix} = \begin{pmatrix} A_{44} & A_{45} \\ A_{45} & A_{55} \end{pmatrix} \begin{pmatrix} w_{,y} + \psi_y \\ w_{,x} + \psi_x \end{pmatrix} \quad (6)$$

here

$$(A_{ij}, B_{ij}, D_{ij}) = \int_{-h/2}^{h/2} \bar{Q}_{ij}(1, z, z^2) dz \quad i, j = 1, 2, 6$$

$$A_{ij} = k' \int_{-h/2}^{h/2} \bar{Q}_{ij} dz \quad i, j = 4, 5 \quad (7)$$

and

$$\begin{pmatrix} N_x^T \\ N_y^T \\ N_{xy}^T \end{pmatrix} = \Delta T \int_{-h/2}^{h/2} \begin{pmatrix} \bar{Q}_{11} & \bar{Q}_{12} & \bar{Q}_{16} \\ \bar{Q}_{12} & \bar{Q}_{22} & \bar{Q}_{26} \\ \bar{Q}_{16} & \bar{Q}_{26} & \bar{Q}_{66} \end{pmatrix}^{(k)} \begin{pmatrix} \alpha_x \\ \alpha_y \\ \alpha_{xy} \end{pmatrix}^{(k)} dz \quad (8)$$

where

$$\begin{pmatrix} \alpha_x \\ \alpha_y \\ \alpha_{xy} \end{pmatrix}^{(k)} = \begin{pmatrix} \cos^2 \theta & \sin^2 \theta \\ \sin^2 \theta & \cos^2 \theta \\ 2 \cos \theta \sin \theta & -2 \cos \theta \sin \theta \end{pmatrix}^{(k)} \begin{pmatrix} \alpha_1 \\ \alpha_2 \end{pmatrix} \quad (9)$$

k' is shear correction factor. A_{ij} , D_{ij} and B_{ij} are extensional stiffness, flexural stiffness, and flexural-extensional coupling stiffness coefficients, and N_x^T , N_y^T and N_{xy}^T are the thermal in-plane forces, respectively. α_1 and α_2 are thermal expansion coefficients in principal directions and θ is the fiber orientation of k th layer (It's measured counter clockwise from x axes).

The equilibrium equations of linear elasticity are (Whitney (1987))

$$\begin{aligned}
N_{x,x} + N_{xy,y} &= 0 \\
N_{xy,x} + N_{y,y} &= 0 \\
M_{x,x} + M_{xy,y} - Q_x &= 0 \\
M_{xy,x} + M_{y,y} - Q_y &= 0 \\
Q_{x,x} + Q_{y,y} + N_x w_{,xx} + 2N_{xy} w_{,xy} + N_y w_{,yy} &= 0
\end{aligned} \quad (10)$$

Substituting N , M , and Q from Eq. (6) into Eq. (10), the equations of equilibrium are derived in terms of displacements and rotations. Under a uniform temperature field, these equations are expressed as follow

$$A_{11}u_{0,xx} + 2A_{16}u_{0,xy} + A_{66}u_{0,yy} + A_{16}v_{0,xx} + (A_{12} + A_{66})v_{0,xy} + A_{26}v_{0,yy} + B_{11}\psi_{x,xx} + 2B_{16}\psi_{x,xy} + B_{66}\psi_{x,yy} + B_{16}\psi_{y,xx} + (B_{12} + B_{66})\psi_{y,xy} + B_{26}\psi_{y,yy} = 0 \quad (11a)$$

$$A_{16}u_{0,xx} + (A_{12} + A_{66})u_{0,xy} + A_{26}u_{0,yy} + A_{66}v_{0,xx} + 2A_{26}v_{0,xy} + A_{22}v_{0,yy} + B_{16}\psi_{x,xx} + (B_{12} + B_{66})\psi_{x,xy} + B_{26}\psi_{x,yy} + B_{66}\psi_{y,xx} + 2B_{26}\psi_{y,xy} + B_{22}\psi_{y,yy} = 0 \quad (11b)$$

$$B_{11}u_{0,xx} + 2B_{16}u_{0,xy} + B_{66}u_{0,yy} + B_{16}v_{0,xx} + (B_{12} + B_{66})v_{0,xy} + B_{26}v_{0,yy} + D_{11}\psi_{x,xx} + 2D_{16}\psi_{x,xy} + D_{66}\psi_{x,yy} + D_{16}\psi_{y,xx} + (D_{12} + D_{66})\psi_{y,xy} + D_{26}\psi_{y,yy} - [A_{55}(\psi_x + w_{0,x}) + A_{45}(\psi_y + w_{0,y})] = 0 \quad (11c)$$

$$B_{16}u_{0,xx} + (B_{12} + B_{66})u_{0,xy} + B_{26}u_{0,yy} + B_{66}v_{0,xx} + 2B_{26}v_{0,xy} + B_{22}v_{0,yy} + D_{16}\psi_{x,xx} + (D_{12} + D_{66})\psi_{x,xy} + D_{26}\psi_{x,yy} + D_{66}\psi_{y,xx} + 2D_{26}\psi_{y,xy} + D_{22}\psi_{y,yy} - [A_{45}(\psi_x + w_{0,x}) + A_{44}(\psi_y + w_{0,y})] = 0 \quad (11d)$$

$$[A_{55}(\psi_{x,x} + w_{0,xx}) + A_{45}(\psi_{x,y} + \psi_{y,x} + 2w_{0,xy}) + A_{44}(\psi_{y,y} + w_{0,yy})] + N_x w_{0,xx} + 2N_{xy} w_{0,xy} + N_y w_{0,yy} = 0 \quad (11e)$$

Using the following non-dimensionalized parameters (Chia (1980))

$$\begin{aligned} X &= \frac{x}{a} & , & & Y &= \frac{y}{b} & , & & U &= \frac{u_0}{a} & , & & V &= \frac{v_0}{b} \\ W &= \frac{w}{h} & , & & \alpha &= \frac{a}{b} & , & & \beta &= \frac{h}{a} & , & & \gamma &= \frac{h}{b} \\ A_{ij}^* &= \frac{A_{ij}}{A_{22}} & , & & B_{ij}^* &= \frac{B_{ij}}{hA_{22}} & , & & D_{ij}^* &= \frac{D_{ij}}{h^2A_{22}} \end{aligned} \quad (12)$$

and applying the DQ method to the Eqs. (11a) to (11e), one can obtain the following system of algebraic equations

$$\begin{aligned}
& A_{11}^* \sum_{k=1}^{n_x} C_{ik}^{(2)} U_{kj} + 2\alpha A_{16}^* \sum_{k=1}^{n_x} C_{ik}^{(1)} \sum_{\ell=1}^{n_y} C_{j\ell}^{(1)} U_{k\ell} + \alpha^2 A_{66}^* \sum_{k=1}^{n_y} C_{jk}^{(2)} U_{ik} + (1/\alpha) A_{16}^* \sum_{k=1}^{n_x} C_{ik}^{(2)} V_{kj} + \\
& (A_{12}^* + A_{66}^*) \sum_{k=1}^{n_x} C_{ik}^{(1)} \sum_{\ell=1}^{n_y} C_{j\ell}^{(1)} V_{k\ell} + \alpha A_{26}^* \sum_{k=1}^{n_y} C_{jk}^{(2)} V_{ik} + \beta B_{11}^* \sum_{k=1}^{n_x} C_{ik}^{(2)} \psi_{xkj} + \\
& 2\gamma B_{16}^* \sum_{k=1}^{n_x} C_{ik}^{(1)} \sum_{\ell=1}^{n_y} C_{j\ell}^{(1)} \psi_{xk\ell} + \alpha\gamma B_{66}^* \sum_{k=1}^{n_y} C_{ik}^{(2)} \psi_{xik} + \beta B_{16}^* \sum_{k=1}^{n_x} C_{ik}^{(2)} \psi_{ykj} + \\
& \gamma (B_{12}^* + B_{66}^*) \sum_{k=1}^{n_x} C_{ik}^{(1)} \sum_{\ell=1}^{n_y} C_{j\ell}^{(1)} \psi_{y k\ell} + \alpha\gamma B_{26}^* \sum_{k=1}^{n_y} C_{jk}^{(2)} \psi_{y ik} = 0
\end{aligned} \tag{13a}$$

$$\begin{aligned}
& A_{16}^* \sum_{k=1}^{n_x} C_{ik}^{(2)} U_{kj} + \alpha (A_{12}^* + A_{66}^*) \sum_{k=1}^{n_x} C_{ik}^{(1)} \sum_{\ell=1}^{n_y} C_{j\ell}^{(1)} U_{k\ell} + \alpha^2 A_{26}^* \sum_{k=1}^{n_y} C_{jk}^{(2)} U_{ik} + \\
& (1/\alpha) A_{66}^* \sum_{k=1}^{n_x} C_{ik}^{(2)} V_{kj} + 2A_{26}^* \sum_{k=1}^{n_x} C_{ik}^{(1)} \sum_{\ell=1}^{n_y} C_{j\ell}^{(1)} V_{k\ell} + \alpha A_{22}^* \sum_{k=1}^{n_y} C_{jk}^{(2)} V_{ik} + \beta B_{16}^* \sum_{k=1}^{n_x} C_{ik}^{(2)} \psi_{xkj} + \\
& \gamma (B_{12}^* + B_{66}^*) \sum_{k=1}^{n_x} C_{ik}^{(1)} \sum_{\ell=1}^{n_y} C_{j\ell}^{(1)} \psi_{x k\ell} + \alpha\gamma B_{26}^* \sum_{k=1}^{n_y} C_{ik}^{(2)} \psi_{x ik} + \beta B_{66}^* \sum_{k=1}^{n_x} C_{ik}^{(2)} \psi_{y kj} + \\
& 2\gamma B_{26}^* \sum_{k=1}^{n_x} C_{ik}^{(1)} \sum_{\ell=1}^{n_y} C_{j\ell}^{(1)} \psi_{y k\ell} + \alpha\gamma B_{22}^* \sum_{k=1}^{n_y} C_{jk}^{(2)} \psi_{y ik} = 0
\end{aligned} \tag{13b}$$

$$\begin{aligned}
& \beta B_{11}^* \sum_{k=1}^{n_x} C_{ik}^{(2)} U_{kj} + 2\gamma B_{16}^* \sum_{k=1}^{n_x} C_{ik}^{(1)} \sum_{\ell=1}^{n_y} C_{j\ell}^{(1)} U_{k\ell} + \alpha\gamma B_{66}^* \sum_{k=1}^{n_y} C_{jk}^{(2)} U_{ik} + \\
& (\beta/\alpha) B_{16}^* \sum_{k=1}^{n_x} C_{ik}^{(2)} V_{kj} + \beta (B_{12}^* + B_{66}^*) \sum_{k=1}^{n_x} C_{ik}^{(1)} \sum_{\ell=1}^{n_y} C_{j\ell}^{(1)} V_{k\ell} + \\
& \gamma B_{26}^* \sum_{k=1}^{n_x} C_{jk}^{(2)} V_{ik} + \beta^2 D_{11}^* \sum_{k=1}^{n_x} C_{ik}^{(2)} \psi_{xkj} + 2\gamma\beta D_{16}^* \sum_{k=1}^{n_x} C_{ik}^{(1)} \sum_{\ell=1}^{n_y} C_{j\ell}^{(1)} \psi_{xk\ell} + \\
& \gamma^2 D_{66}^* \sum_{k=1}^{n_y} C_{ik}^{(2)} \psi_{x ik} + \beta^2 D_{16}^* \sum_{k=1}^{n_x} C_{ik}^{(2)} \psi_{y kj} + \\
& \beta\gamma (D_{12}^* + D_{66}^*) \sum_{k=1}^{n_x} C_{ik}^{(1)} \sum_{\ell=1}^{n_y} C_{j\ell}^{(1)} \psi_{y k\ell} + \gamma^2 D_{26}^* \sum_{k=1}^{n_y} C_{jk}^{(2)} \psi_{y ik} - \\
& \left[A_{55}^* \left(\psi_{x ij} + \beta \sum_{k=1}^{n_x} C_{ik}^{(1)} W_{kj} \right) + A_{45}^* \left(\psi_{y ij} + \gamma \sum_{k=1}^{n_y} C_{jk}^{(1)} W_{ik} \right) \right] = 0
\end{aligned} \tag{13c}$$

$$\begin{aligned}
& \beta B_{16}^* \sum_{k=1}^{n_x} C_{ik}^{(2)} U_{kj} + \gamma (B_{12}^* + B_{66}^*) \sum_{k=1}^{n_x} C_{ik}^{(1)} \sum_{\ell=1}^{n_y} C_{j\ell}^{(1)} U_{k\ell} + \alpha \gamma B_{26}^* \sum_{k=1}^{n_x} C_{jk}^{(2)} U_{ik} + \\
& (\beta / \alpha) B_{66}^* \sum_{k=1}^{n_x} C_{ik}^{(2)} V_{kj} + 2\beta B_{26}^* \sum_{k=1}^{n_x} C_{ik}^{(1)} \sum_{\ell=1}^{n_y} C_{j\ell}^{(1)} V_{k\ell} + \\
& \gamma B_{22}^* \sum_{k=1}^{n_y} C_{jk}^{(2)} V_{ik} + \beta^2 D_{16}^* \sum_{k=1}^{n_x} C_{ik}^{(2)} \psi_{xkj} + \gamma \beta (D_{12}^* + D_{66}^*) \sum_{k=1}^{n_x} C_{ik}^{(1)} \sum_{\ell=1}^{n_y} C_{j\ell}^{(1)} \psi_{xk\ell} + \\
& \gamma^2 D_{26}^* \sum_{k=1}^{n_y} C_{ik}^{(2)} \psi_{xik} + \beta^2 D_{66}^* \sum_{k=1}^{n_x} C_{ik}^{(2)} \psi_{ykj} + \\
& 2\beta \gamma D_{26}^* \sum_{k=1}^{n_x} C_{ik}^{(1)} \sum_{\ell=1}^{n_y} C_{j\ell}^{(1)} \psi_{y k\ell} + \gamma^2 D_{22}^* \sum_{k=1}^{n_y} C_{jk}^{(2)} \psi_{yik} - \\
& \left[A_{45}^* \left(\psi_{xij} + \beta \sum_{k=1}^{n_x} C_{ik}^{(1)} W_{kj} \right) + A_{44}^* \left(\psi_{yij} + \gamma \sum_{k=1}^{n_y} C_{jk}^{(1)} W_{ik} \right) \right] = 0
\end{aligned} \tag{13d}$$

$$\begin{aligned}
& A_{55}^* \left(\sum_{k=1}^{n_x} C_{ik}^{(1)} \psi_{xkj} + \beta \sum_{k=1}^{n_x} C_{ik}^{(2)} W_{kj} \right) + A_{45}^* \left(\alpha \sum_{k=1}^{n_y} C_{jk}^{(1)} \psi_{xkj} + \sum_{k=1}^{n_x} C_{ik}^{(1)} \psi_{y kj} + \right. \\
& \left. 2\gamma \sum_{k=1}^{n_x} C_{ik}^{(1)} \sum_{\ell=1}^{n_y} C_{j\ell}^{(1)} W_{k\ell} \right) + A_{44}^* \left(\alpha \sum_{k=1}^{n_y} C_{jk}^{(1)} \psi_{yik} + \alpha \gamma \sum_{k=1}^{n_y} C_{jk}^{(2)} W_{ik} \right) + \\
& \beta \frac{N_x(x_i, y_j)}{A_{22}} \sum_{k=1}^{n_x} C_{ik}^{(2)} W_{kj} + 2\gamma \frac{N_{xy}(x_i, y_j)}{A_{22}} \sum_{k=1}^{n_x} C_{ik}^{(1)} \sum_{\ell=1}^{n_y} C_{j\ell}^{(1)} W_{k\ell} + \\
& \alpha \gamma \frac{N_y(x_i, y_j)}{A_{22}} \sum_{k=1}^{n_y} C_{jk}^{(2)} W_{ik} = 0
\end{aligned} \tag{13e}$$

$$i = 2, 3, \dots, (n_x - 1) \quad , \quad j = 2, 3, \dots, (n_y - 1)$$

where $N_x(x_i, y_j)$, $N_y(x_i, y_j)$ and $N_{xy}(x_i, y_j)$ are membrane pre-buckling forces, which for the pre-buckling analysis should be determined. For the buckling analysis they are known functions obtained from the pre-buckling analysis.

The thermal load creates in-plane compressive forces that cause the buckling of the plate. In order to find the critical buckling temperature, it is important to determine these pre-buckling in-plane forces. Therefore, the analysis takes place in two separate steps. First, pre-buckling forces are determined by using a membrane solution at arbitrary temperature. The magnitude of the temperature can be defined with respect to a temperature factor λ . The plate remains flat at this state, so the quantities of w , ψ_x and ψ_y are set to zero. The solution of the first two equations of (13) along with the corresponding boundary conditions, which will be discussed later, give the pre-buckling in-plane displacements, forces and thermal stresses.

The flat laminated plate is acted upon by the pre-buckling membrane stresses, which are computed in

previous step. The aim now in the second step of the analysis is to determine, in the context of well-known Reissner-Mindlin first-order shear deformation theory, the critical temperature that causes the buckling of plate. At the buckling, all displacements and other quantities derived from them are assumed to be occurred at constant temperature. Therefore, it should be noted that there are no thermal in-plane forces, N^T , in this step.

The following boundary conditions have been used in this study:
simply supported immovable edges, S1

$$\begin{aligned} u_0 = v_0 = w_0 = \psi_y = M_x = 0 \quad \text{at } x = 0, a \\ u_0 = v_0 = w_0 = \psi_x = M_y = 0 \quad \text{at } y = 0, b \end{aligned} \quad (14a)$$

simply supported movable edges (in normal direction), S2

$$\begin{aligned} v_0 = w_0 = \psi_y = M_x = N_x = 0 \quad \text{at } x = 0, a \\ u_0 = w_0 = \psi_x = M_y = N_y = 0 \quad \text{at } y = 0, b \end{aligned} \quad (14b)$$

simply supported movable edges (in tangential direction), S3

$$\begin{aligned} u_0 = w_0 = \psi_y = M_x = N_y = 0 \quad \text{at } x = 0, a \\ v_0 = w_0 = \psi_x = M_y = N_x = 0 \quad \text{at } y = 0, b \end{aligned} \quad (14c)$$

clamped immovable edges, C1

$$u_0 = v_0 = w_0 = \psi_y = \psi_x = 0 \quad \text{at } x = 0, a \quad \text{and} \quad y = 0, b \quad (14d)$$

These boundary conditions can be placed to the first point around the boundaries of Eqs. (13a) to (13e). Then, combining the equilibrium equations along with the corresponding boundary conditions gives an eigenvalue problem. The solution of this eigenvalue problem by a standard eigensolver provides the critical temperature.

3. Numerical results and discussion

The formulation presented in the preceding section was implemented into a computer code for evaluating the thermal buckling response of a composite laminated plate as shown in Fig. 1. To show the validity of DQ method for the selected application, several case studies were investigated. In all cases, the temperature distribution was assumed to be uniform, boundary conditions had the same type on all four edges and shear correction factor k' was $5/6$.

To verify the validity of DQ method, the critical temperature of a thin square isotropic plate under different boundary conditions are compared with the results obtained by the Finite Element Method

(FEM) (Thangaratnam *et al.* (1989)) and the Finite Strip Method (FSM) (Dawe and Ge (2000)), as shown in Table 1. Different number of sampling points has been used to obtain the critical buckling temperature of S3 and C1 plates. As can be seen from the table the DQ method converges quickly, good agreement stands amongst the results and deviations are negligible. The table also shows the effect of the number of sampling points on the convergence of the buckling temperature.

3.1 Symmetric laminates

The results of the DQ method for a square single-layer plate subject to a uniform thermal field are compared with those of FEM (Huang and Tauchert (1992)), FSM (Dawe and Ge (2000)), and Fourier series method (Huang and Tauchert (1992)), as presented in Table 2. The material properties of the plate are listed in Table 3. The first set of the material properties have been selected for this case study.

Table 1. Critical temperatures of square isotropic plate ($a/h = 100$, $\nu = 0.3$, $\alpha = 2 \times 10^6$)

Solution Method	$n_x \times n_y$	T_{cr} (°C)	
		S3	C1
Present - DQ	5×5	62.13	187.71
	6×6	62.30	188.58
	7×7	63.25	167.46
	8×8	63.25	167.44
	9×9	63.23	167.48
	10×10	63.23	167.48
	11×11	63.23	167.48
FEM (Thangaratnam <i>et al.</i> (1989))		63.33	167.70
FSM (Dawe and Ge (2000))		63.22	167.5

Table 2. Critical temperatures of square single-layer plate with C1 boundary conditions and material property set 1 – ($b/h = 40$)

Solution Method	T_{cr} (°C)	
	$\theta = 0^\circ$	$\theta = 45^\circ$
DQ - (11×11)	152.19	129.99
Fourier series (Huang and Tauchert (1992))	152.47	131.88
FEM (Huang and Tauchert (1992))	152.30	129.91
FSM (Dawe and Ge (2000))	151.2	129.3

Table 3. Orthotropic material properties

Material Set ^a	$\frac{E_1}{E_o}$	$\frac{E_2}{E_o}$	$\frac{G_{12}}{E_o}$	$\frac{G_{13}}{E_o}$	$\frac{G_{23}}{E_o}$	ν_{12}	$\frac{\alpha_1}{\alpha_o}$	$\frac{\alpha_2}{\alpha_o}$
1	76	5.5	2.3	2.3	1.5	0.34	-4	79
2	40	1	0.6	0.6	0.5	0.25	0.02	22.5
3	181	10.3	7.17	5.98	2.39	0.28	0.02	22.5
4	40	1	0.6	0.6	0.5	0.25	1	2

a $E_o = 10^5 \text{GPa}$, $\alpha_o = 10^{-6} / ^\circ\text{C}$

Here a 11×11 grid spacing was used to discretize the domain. The comparison of the results shows a good agreement between the DQ and the aforementioned methods. However, the DQ results are closer to the results obtained by FEM compare with those of the FSM and Fourier series method.

The effect of grid spacing on the buckling temperature was also investigated for the squared single-layer plate with lamina fiber angle equal to zero, presented in the previous case study. Here we examine the effect of grid spacing through the use of the following sets of sampling points in the normalized region $[0,1]$

$$x_i = \left\{ \frac{i-1}{n_x-1} \right\}, \quad i = 1, 2, \dots, n_x \quad (15)$$

$$x_i = \left\{ 0, \frac{1}{2} \left(1 - \cos\left(\frac{2i-1}{2(n_x-2)}\pi\right) \right), 1 \right\}, \quad i = 1, 2, \dots, (n_x - 2) \quad (16)$$

$$x_i = \left\{ 0, (n_x - 2) \text{ zeros of shifted legendre polynomial}, 1 \right\}, \quad i = 2, \dots, (n_x - 1) \quad (17)$$

$$x_i = \left\{ \frac{1}{2} \left(1 - \cos\left(\frac{i-1}{n_x-1}\pi\right) \right) \right\}, \quad i = 1, 2, \dots, n_x \quad (18)$$

where the first scheme is based on the uniform spacing, and the others are referred to as the zeros of the shifted Chebyshev, Legendre, and Chebyshev-Gauss-Lobatto polynomials, respectively. Similar spacing schemes for the sampling points were used in the y direction. Fig. 3 illustrates the performance of the above grid spacing for different number of sampling points. As can be seen from the figure, the

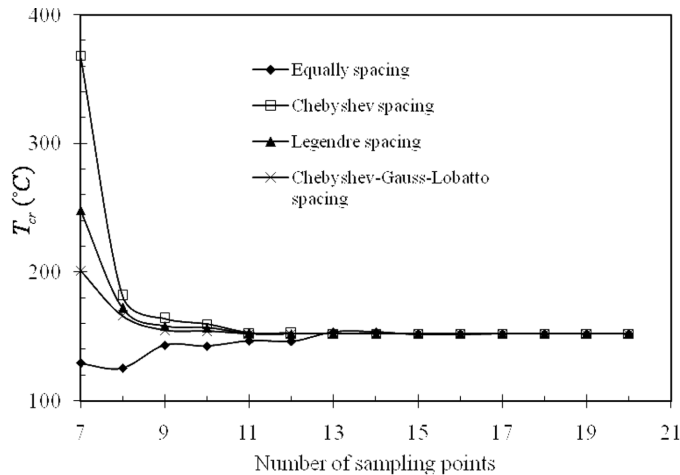


Fig. 3 Convergence of DQ method with different grid spacing schemes

critical buckling temperature for all grid spacing schemes converged rapidly to the solution. Moreover, using Chebyshev-Gauss-Lobatto sampling points produces the best convergence among all the schemes. Therefore, for the rest of this study we used this scheme.

To study the effects of fiber orientation on the thermal buckling, a five-layer laminated symmetric plate ($\theta/\theta/\theta/\theta/\theta$) with different aspect ratios is considered for investigation. The material properties of the lamina are the same as set 2 in Table 3. The critical temperature for the plate, which is subjected to a uniform temperature field, is calculated and compared with those of FEM and FSM.

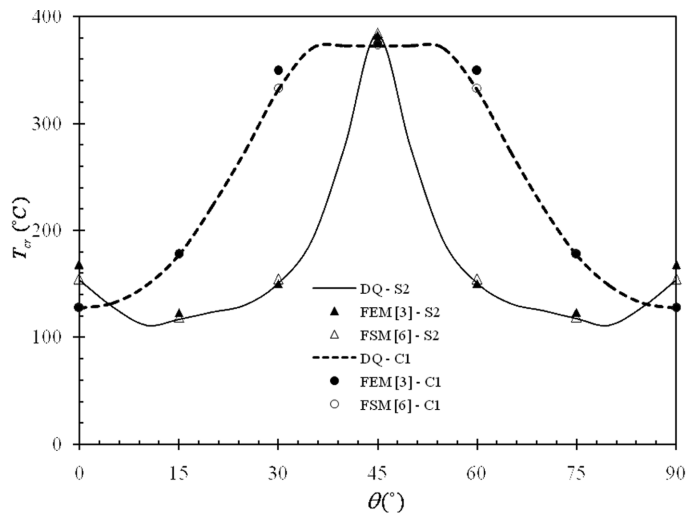


Fig. 4 Variation of critical temperature with fiber orientation for thin square, symmetric angle-ply laminates with C1 and S2 boundary conditions – ($a/b = 1$, $b/h = 100$). ([3]=Prabhu and Dhanaraj (1994), [6]=Dawe and Ge (2000))

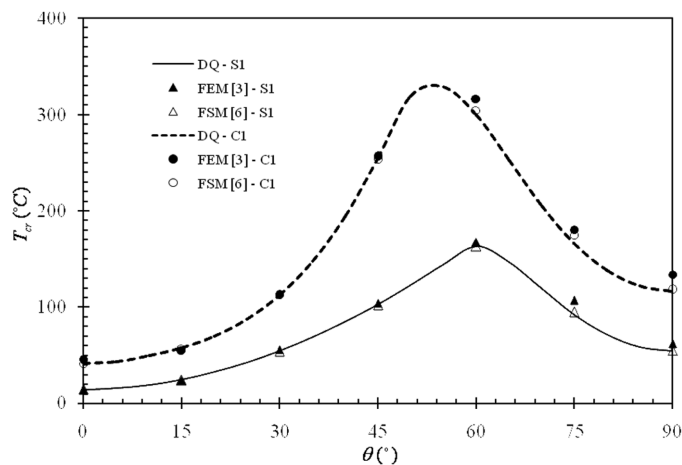


Fig. 5 Variation of critical temperature with fiber orientation for thin rectangular, symmetric angle-ply laminates with C1 and S1 boundary conditions – ($a/b = 2$, $b/h = 100$). ([3]=Prabhu and Dhanaraj (1994), [6]=Dawe and Ge (2000))

Figs. 4 and 5 show the results of the critical temperature for a thin plate under simply supported and clamped boundary conditions. The lamina fiber angle is successively rotated from 0° to 90° (with respect to the longitudinal, x -axis). As seen in the figures, the DQ results agree well with those of FSM and FEM. Moreover, in Fig. 4, the buckling temperature has a large variation around $\theta = 45^\circ$ for S2 and C1 boundary conditions of an squared plate, while for the plate with aspect ratio of two, the maximum buckling temperature occurs at $0^\circ = 60^\circ$ for S1 boundary conditions and at around $\theta = 55^\circ$ for C1 boundary conditions. These results are in agreement with those in (Prabhu and Dhanaraj (1994), Dawe and Ge (2000)).

Figs. 6 to 9 show the effect of different modulus ratios on the critical buckling temperature of thick

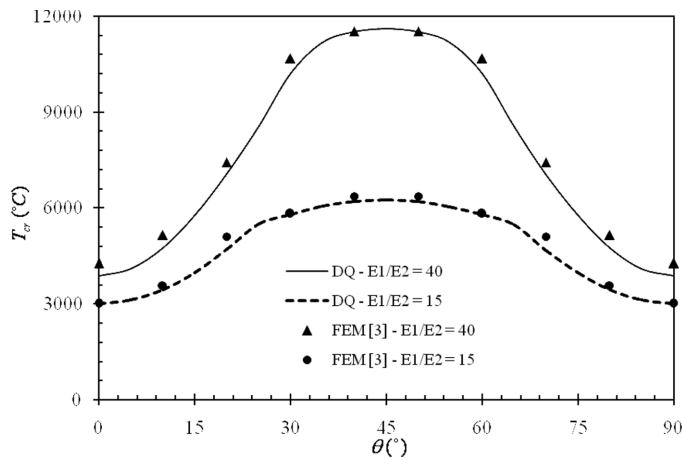


Fig. 6 Variation of critical temperature with fiber orientation for thick square, symmetric angle-ply laminates with S1 boundary condition – ($a/b = 1$, $b/h = 10$). ([3]=Prabhu and Dhanaraj (1994))

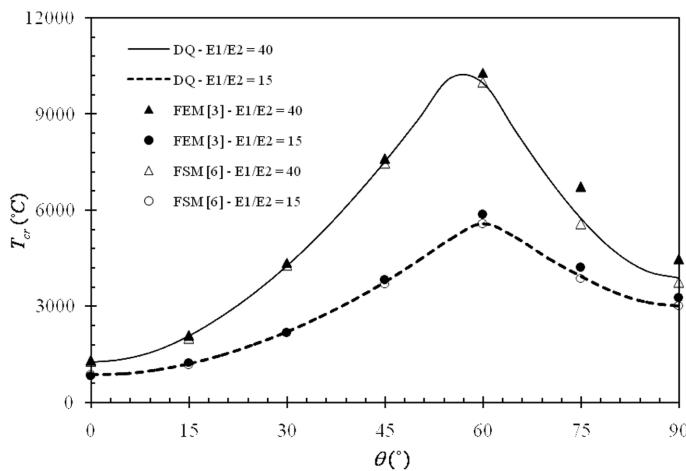


Fig. 7 Variation of critical temperature with fiber orientation for thick rectangular, symmetric angle-ply laminates with S1 boundary condition – ($a/b = 2$, $b/h = 10$). ([3]=Prabhu and Dhanaraj (1994), [6]=Dawe and Ge (2000))

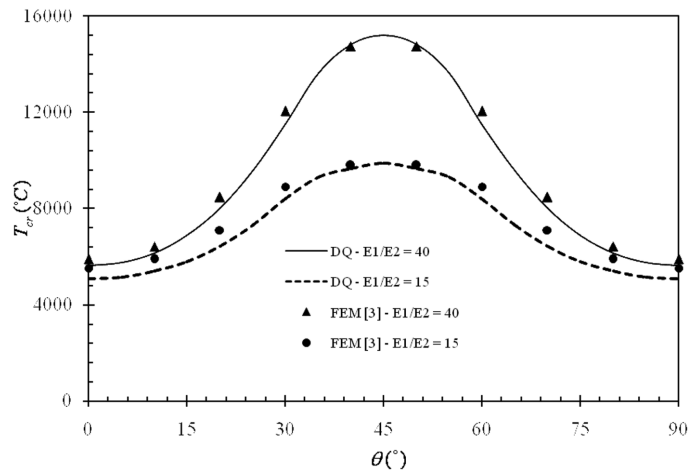


Fig. 8 Variation of critical temperature with fiber orientation for thick square, symmetric angle-ply laminates with C1 boundary condition – ($a/b = 1$, $b/h = 10$). ([3]=Prabhu and Dhanaraj (1994))

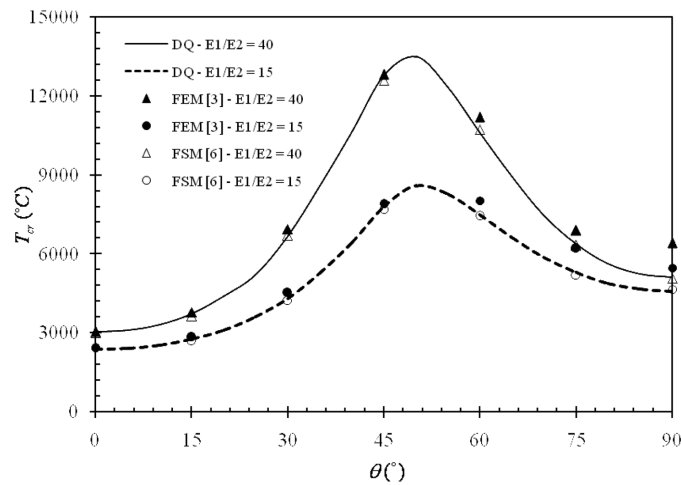


Fig. 9 Variation of critical temperature with fiber orientation for thick rectangular, symmetric angle-ply laminates with C1 boundary condition – ($a/b = 2$, $b/h = 10$). ([3]=Prabhu and Dhanaraj (1994), [6]=Dawe and Ge (2000))

symmetric angle-ply plates. As seen from these figures, the DQ results are in good agreement with those of FEM and particularly with FSM. Increasing modulus ratio would result in an increase in the overall buckling temperature. Furthermore, the maximum critical temperature occurs at the 45-degree fiber orientation for squared thin or thick plates.

The DQ results for five-layers square symmetric cross-ply plate, (0/90/0/90/0), under simply-supported and clamped boundary conditions with material property set 2, are compared with those of FEM in Fig. 10. As can be seen, good agreement stands between the results. The figure also shows that reduction in the thickness of the plate results in a drastic reduction of critical temperature.

Table 4. Critical temperatures of antisymmetric angle-ply plates with S3 boundary conditions and material property set 3 – ($a/h = 20$).

a/b	Lay-up ^a	T_{cr} (°C)		
		DQ – (9 × 9)	FSM, Type 1*	FSM, Type 2*
1/2	[26.9/-31.4] _a	1841.23	1834	1841
2/3	[25.5/-31.9] _a	1856.54	1849	1857
1	[45/-45] _a	2032.55	2025	2033
3/2	[-64.5/58.3] _a	3735.43	3697	3735
2	[-63.1/58.6] _a	5938.29	5849	5938

a [θ_1/θ_2]_a ≡ ($\theta_1/\theta_2/-\theta_2/-\theta_1$)

*(Dawe and Ge (2000))

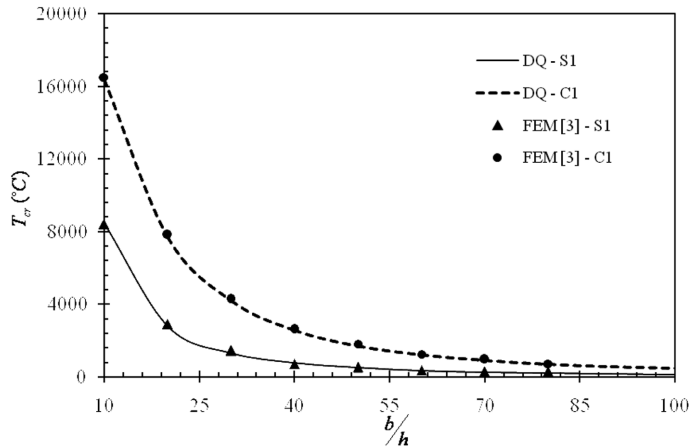


Fig. 10 Variation of critical temperature with b/h ratio for square symmetric cross-ply laminates with S1 and C1 boundary condition – ($a/b = 1$, $E_1/E_2 = 40$). ([3]=Prabhu and Dhanaraj (1994))

3.2 Anti-symmetric laminates

The bifurcation buckling analysis can be used to analyze anti-symmetric angle-ply and cross-ply laminated plates. The results of the application of DQ method to the thermal buckling analysis of anti-symmetric angle-ply composite plates for different fiber angles and aspect ratios are tabulated in Table 4. In this table the DQ results, obtained by a 11×11 grid points, are compared with those of Dawe and Ge (2000). They used the FSM to analyze the thermal buckling problem of composite plates. In order to obtain the buckling temperature, they used a pre-buckling analysis followed by a buckling analysis using Reissner-Mindlin first order SDPT.

The results of FSM are presented for two different types of formulation. The first type considers the full expression for potential energy of the pre buckling stresses, while the second type uses a reduced and approximate expression. As seen from this table, the results of the DQ method are in excellent agreement with type 2 FSM results of Dawe and Ge (2000), while showing a small difference with those of type 1.

Figs. 11 and 12 show the results of the DQ, FEM and FSM for square anti-symmetric angle-ply plates

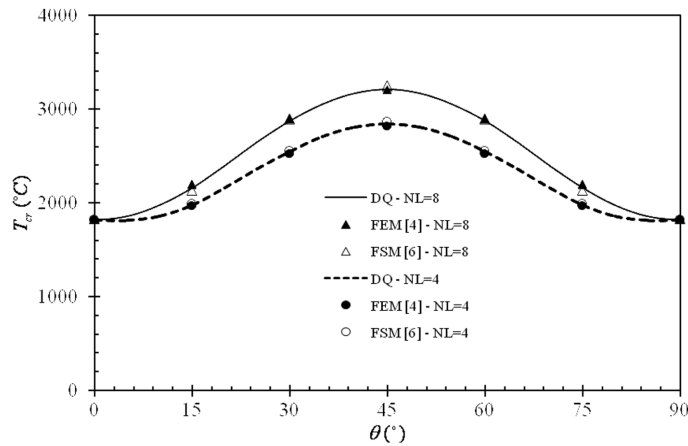


Fig. 11 Variation of critical temperature with fiber orientation for thick square, antisymmetric angle-ply laminates with S3 boundary condition $(a/b = 1, a/h = 20)$. ([3]=Prabhu and Dhanaraj (1994), [6]=Dawe and Ge (2000))

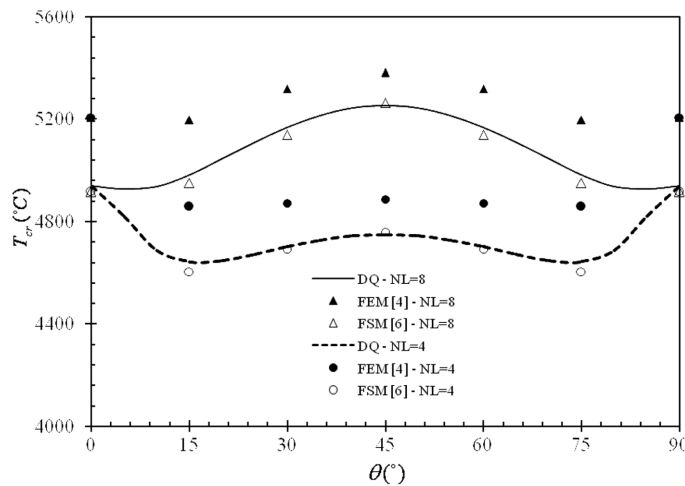


Fig. 12 Variation of critical temperature with fiber orientation for thick square, antisymmetric angle-ply laminates with C1 boundary condition $(a/b = 1, a/h = 20)$. ([3]=Prabhu and Dhanaraj (1994), [6]=Dawe and Ge (2000))

subjected to a uniform thermal field under simply supported and clamped boundary conditions. The plates have 4 and 8 layers in the form of $(\theta/-\theta)$ layup with constant thickness and material property set 4. The figures show that there are an excellent agreement between these methods for the simply supported plates, while the results of FEM have some differences compare with those of DQ and FSM for the clamped plates. In this case, the FEM predicts higher quantities, particularly for the 0 and 90 deg. lamina angles. For anti-symmetric square plates, similar to symmetric angle-ply plates, the critical temperature variations are symmetric with respect to 45 deg. lamina angle. The critical temperatures of a square antisymmetric cross-ply composite plate, under clamped boundary conditions, for different aspect ratios are shown in Table 5.

Table 5. Critical temperatures of antisymmetric cross-ply plates, (0/90/0/90), with C1 boundary conditions and material property set 3 – ($b/h = 20$)

a/b	T_{cr} (°C)	
	DQ – (11×11)	FSM *
1/2	8686.55	8562
2/3	6169.27	6101
1	3942.07	3909
3/2	3264.41	3242
2	3131.59	3113

*(Dawe and Ge (2000))

4. Conclusions

In this study the application of DQ method to the thermal buckling analysis of laminated composite plates were investigated. The critical load was obtained under a uniform temperature distribution and arbitrary boundary conditions. A pre-buckling membrane analysis followed by an eigenvalue analysis based on FSDT was used to find the critical buckling temperature. Several case studies were investigated to establish the applicability and the integrity of the proposed methodology. These included the symmetric and anti-symmetric thin and thick composite plates with different boundary conditions. The results validate the applicability of the method for solving such engineering problems. The method provides accurate results with relatively minimal computational and modeling efforts.

References

- Bellman, R. and Casti, J. (1971), "Differential quadrature and long-term integration", *J. Math. Anal. Appl.* **10**, 235-238.
- Bert, C.W. and Malik, M., (1996), "Differential quadrature method in computational mechanics: A review", *Appl. Mech. Rev.*, **49**(1), 1-28.
- Chen, W.J., Lin, P.D. and Chen, L.W. (1991), "Thermal buckling behavior of thick composite laminated plates under nonuniform temperature distribution", *Comput. Struct.* **41**(4), 637-645.
- Chia, C.Y. (1980), *Nonlinear analysis of plates*, McGraw-Hill, New York.
- Dawe, D.J. and Ge, Y.S. (2000), "Thermal buckling of shear-deformable composite laminated plates by the spline finite strip method", *Comput. Method. Appl. Mech. Eng.*, **185**(2-4), 347-366.
- Farid, M., Zahedinejad, P. and Malekzadeh, P. (2010), "Three-dimensional temperature dependent free vibration analysis of functionally graded material curved panels resting on two-parameter elastic foundation using a hybrid semi-analytic, differential quadrature method", *Mater. Design*, **31**(1), 2-13.
- Hakimi, H. and Moradi, S. (2010), "Drillstring vibration analysis using differential quadrature method", *J. PETROL. SCI. ENG.* **70**(3-4), 235-242.
- Hong, C.C. and Jane, K.C. (2003), "Shear deformation in thermal bending analysis of laminated plates by the GDQ method", *Mech. Res. Commun.*, **30**(2), 175-186.
- Hu, Y.J., Zhu, Y.Y. and Cheng, C.J. (2009), "DQM for dynamic response of fluid-saturated visco-elastic porous media", *Inter. J. Solid. Struct.*, **46**(7-8), 1667-1675.
- Huang, N.N. and Tauchert, T.R. (1992), "Thermal buckling of clamped symmetric laminated plates", *J. Thin-Wall. Struct.*, **13**(4), 259-273.
- Jane, K.C. and Hong, C.C. (2000), "Thermal bending analysis of laminated orthotropic plates by the generalized differential quadrature method", *Mech. Res. Commun.*, **27**(2), 157-164.

- Kabir, H.R.H., Hamad, M.A.M., Al-Duaij, J. and John, M.J. (2007), "Thermal buckling response of all-edge clamped rectangular plates with symmetric angle-ply lamination". *Compos. Struct.*, **79**(1), 148-155.
- Kant, T. and Babu, C.S., (2000), "Thermal buckling analysis of skew fiber-reinforced composite and sandwich plates using shear deformable finite element models", *Compos. Struct.*, **49**(1), 77-85.
- Karami, G. and Malekzadeh, P., (2006), "DQM free vibration analysis of moderately thick symmetric laminated plates with elastically restrained edges", *Compos. Struct.*, **74**(1), 415-442.
- Leissa, A.W. (1986), "Conditions for laminated plates to remain flat under inplane loading", *Compos. Struct.*, **6**(4), 261-270.
- Li, J.J. and Cheng, C.J. (2005), "Differential quadrature method for nonlinear vibration of orthotropic plates with finite deformation and transverse shear effect", *J. Sound. Vib.*, **281**(1-2), 295-305.
- Lin, R.M., Lim, M.K. and Du, H. (1994), "Large deflection analysis of plates under thermal loading", *Comput. Meth. Appl. Mech. Eng.*, **117**(3-4), 381-390.
- Matsunaga, H. (2006), "Thermal buckling of angle-ply laminated composite and sandwich plates according to a global higher-order deformation theory", *Compos. Struct.*, **72**(2), 177-192.
- Matsunaga, H. (2007), "Thermal buckling of cross-ply laminated composite shallow shells according to a global higher-order deformation theory", *Compos. Struct.*, **81**(2), 210-221.
- Prabhu, M.R. and Dhanaraj, R. (1994), "Thermal buckling of laminated composite plates", *Comput. Struct.*, **53**(5), 1193-1204.
- Prakash, T., Singh, M.K. and Ganapathi, M. (2006), "Vibrations and thermal stability of functionally graded spherical caps", *Struct. Eng. Mech.*, **24**(4), 447-462.
- Qatu, M.S. and Leissa, A.W. (1993), "Buckling or transverse deflections of unsymmetrically laminated plates subjected to in-plane loads", *AIAA Journal*, **31**(1), 189-194.
- Shariyat, M. (2007), "Thermal buckling analysis of rectangular composite plates with temperature-dependent properties based on a layerwise theory", *Thin-Wall. Struct.*, **45**(4), 439-452.
- Shiau, L.C., Kuo, S.Y. and Chen, C.Y. (2010), "Thermal buckling behavior of composite laminated plates", *Compos. Struct.*, **92**(2), 508-514.
- Shu, C. and Richards, B.E., (1992), "Application of generalized differential quadrature to solve two-dimensional incompressible Navier-Stokes equations", *Int. J. Numer. Meth. Fluids*, **15**(7), 791-798.
- Sun, L.X. and Hsu, T.R. (1990), "Thermal buckling of laminated composite plates with transverse shear deformation", *Compu. Struct.*, **36**(5), 883-889.
- Thangaratnam, K.R., Palaninathan, J. and Ramachandran, J. (1989), "Thermal buckling of composite laminated plates", *Comput. Struct.*, **32**(5), 1117-1124.
- Whitney, J.M. (1987), *Structural analysis of laminated anisotropic plates*, Technomic, Lancaster, USA.

CC

Appendix A. A review of differential quadrature method

Bellman and Casti (1971) introduced the DQ method for solving linear or nonlinear differential equations. The method states that the partial derivative of a function with respect to a space variable can be approximated by a weighted linear combination of function values at some intermediate points in the domain of that variable. To show the mathematical representation of DQ method, consider a function $f = f(x, y)$; the r th-order derivative of function f with respect to x , the s th-order derivative of function f with respect to y and the $r+s$ th-order derivative of function f with respect to both x and y at an intermediate discrete point identified by coordinates x_i and y_j can be approximated by the weighted linear sum of the function values as:

$$\begin{aligned} \frac{\partial^r f(x_i, y_j)}{\partial x^r} &= \sum_{k=1}^{n_x} c_{ik}^{(r)} \cdot f(x_k, y_j) \\ \frac{\partial^s f(x_i, y_j)}{\partial y^s} &= \sum_{k=1}^{n_y} c_{jk}^{(s)} \cdot f(x_i, y_k) \quad , \quad r = 1, \dots, n_x - 1 \quad , \quad s = 1, \dots, n_y - 1 \quad (\text{A.1}) \\ \frac{\partial^{(r+s)} f(x_i, y_j)}{\partial x^r \partial y^s} &= \sum_{k=1}^{n_x} c_{ik}^{(r)} \sum_{\ell=1}^{n_y} c_{j\ell}^{(s)} \cdot f(x_k, y_\ell) \end{aligned}$$

Here, the domain is divided into n_x discrete points (sampling points) in the x direction and n_y in the y direction. $c_{ij}^{(r)}$ and $c_{ij}^{(s)}$ are the weighting coefficients of the r th and the s th order partial derivative of f with respect to x and y , respectively. The weighting coefficients may be determined explicitly once and for all discrete points, irrespective of the position and number of sampling points as proposed by Shu and Richards (1992). They used Lagrange interpolating function as the test function and derived the following recurrence formulae for the weighting coefficients

$$\begin{aligned} c_{ij}^{(1)} &= \frac{\prod(x_i)}{(x_i - x_j) \cdot \prod(x_j)} \quad i, j = 1, \dots, n \quad \text{and} \quad j \neq i \\ c_{ij}^{(k)} &= k \left[c_{ii}^{(k-1)} \cdot c_{ij}^{(1)} - \frac{c_{ij}^{(k-1)}}{x_i - x_j} \right] \quad 2 \leq k \leq n-1 \quad (\text{A.2}) \\ c_{ii}^{(m)} &= - \sum_{\substack{j=1 \\ j \neq i}}^n c_{ij}^{(m)} \quad m = 1, \dots, n-1 \end{aligned}$$

where

$$\prod(x_i) = \prod_{\substack{j=1 \\ j \neq i}}^n (x_i - x_j) \quad (\text{A.3})$$

The above relations are not affected by the number of sampling points and thus, significantly reduce the computational effort.